# Six-state, three-level, six-fold ferromagnetic wire system

T. Blachowicz[1a] and A. Ehrmann[2]

[1]*Institute of Physics, Silesian University of Technology, 44-100 Gliwice, Poland*

[2]*Faculty of Textile and Clothing Technology, Niederrhein University of Applied Sciences, 41065 Mönchengladbach, Germany*

Six stable states at remanence were identified in iron wire samples of 6-fold spatial symmetry using micromagnetic simulations and finite element method. Onion and domain-wall magnetic states were tailored by sample shape and guided by an applied magnetic field with a fixed in-plane direction. Different directions of externally applied magnetic fields revealed a tendency for stability or nonstability of the considered states.

PACS numbers: 75.60, 75.78.Cd, 75.75.Jn, 75.75.Fk
Keywords: nano-wires, magnetic anisotropies, magnetization reversal, onion state

[a] Corresponding author: tomasz.blachowicz@polsl.pl

## I. INTRODUCTION

The demand for high-density memories has generated a need for multilevel random access magnetic cells. Magnetoresistive random access memory (MRAM)[1] cells, in their principle of working, are based on magnetization reversal in carefully selected sets of thin layers. A fundamental element of the memory cell is a spin-valve composed from a free magnetic layer, a nonmagnetic spacer, and an exchange-biased ferromagnetic layer[2] or built from two ferromagnetic layers of different magnetic hardness imposed by their thickness.[3] By a sequential addition of such elementary spin-valve sets, it was possible to obtain the two-level four-state[4] and the three-level six-state[5] MRAM cell, respectively.

A similar goal, based on magnetic non-volatility, leading to multiple information storage levels, can be reached in ferromagnetic wire systems.[6] In a set of four iron (Fe) wires with diameter 10 nm and length 70 nm, in the form of a square set, four stable states at remanence were realized. While for layered spin-valve solutions electron transport properties are crucial,[7] for the wire systems shape properties tailored by a length-to-diameter ratio and edge connections are of basic importance. Additionally, while magnetic thin layers can lead to spin-valve effects, the wire solutions are naturally suited for patterned storage media applications.

In our paper we report further efforts for multilevel magnetic data storage objects providing the concept of a magnetic cell (particle) with six distinguishable stable magnetic states at remanence. A particle is built from Fe wires and hexagonally shaped with 70 nm side length. Each side consists of a half-cylinder of 10 nm base width (diameter), while all six wires are coupled at the ends by half-balls of 20 nm diameter (Fig. 1). A sample covers roughly $1.5 \cdot 10^4$ nm$^2$ area, which is comparable with solutions found in MRAM applications.[5]

## II. MODELING

Magpar micromagnetic simulator[8] based on the Landau-Lifshitz-Gilbert (LLG)[9] equation of magnetization vector motion was applied to obtain hysteresis curves for a time-sequence of externally applied magnetic field given in Fig. 2a. A tetrahedral mesh was prepared with the GiD graphical processor (ICNME, Barcelona, Spain) giving information about all nodal mesh-points, where the LLG equation is solved and the values of magnetization, demagnetizing field and energy, exchange field and energy, anisotropy field and energy are calculated. A sample was designed with tetrahedrons of an elementary edge length equal to 3.5 nm. The other material parameters were chosen as follows: exchange constant $A = 2 \cdot 10^{-11}$ J/m, magnetic polarization at saturation $J_s = 2.1$ T, and the

phenomenological Gilbert damping constant $\alpha$ = 0.1. Similarly to our previous efforts,[6] the field sweeping rate of 10 kA/(m·ns) was chosen as typical to that used in MRAM operations.[10] Importantly, using this rate no ripples during magnetization reversal were observed, indicating again an advantage of wire systems compared to typical thin-layer solutions.[11]

## III. RESULTS

In Figs. 2b-2c hysteresis curves for three different in-plane orientations (comp. Fig. 1a) of the externally applied magnetic field are given, for $\alpha = 35°$, and $\alpha = 46°$, respectively. In order to test the stability of the intermediate states, the loops were performed as shown in Fig. 2a: Starting from positive saturation (+500 kA/m), the external magnetic field is decreased until at -140 kA/m the first step in the hysteresis loop is reached. Going back to zero field leads to a new magnetic state (f) different from state (a). Increasing the negative field again causes a second step in the hysteresis loop at -200 kA/m, after which the field is again decreased to zero, leading to a third magnetic state (d) at zero field. Afterwards, the field is driven to negative saturation. The same process now starts with reversed direction of an externally applied magnetic field.

The case seen in Fig. 2b, provides 6 stable states, located symmetrically, which can be arranged in the following pairs: a-b, c-d, and e-f. Obviously, the sample can indeed exist in six different magnetic states, i.e. six different magnetization values, without an external field. Decreasing the magnetic field to zero is a *reversible* process here. This situation is called a "stable intermediate state". A numerical accuracy for the zero-valued magnetic field, for these specific moments, equals to about $4.5 \cdot 10^{-3}$kA/m.

Other sample orientations, such as for example 46°, show a different behavior (Fig. 2c): After decreasing the external magnetic field to zero, the hysteresis loops show *irreversible* parts, i.e. sudden jumps into different magnetic states, recognizable by "closed loops" during the field sweeping process. These irreversible parts indicate clearly that the intermediate magnetic states which are taken during the steps are *not* stable, i.e. they do not exist in the absence of an external magnetic field.

In order to understand this mechanism, spatial distributions of magnetization vector were calculated and visualized (Fig. 3). These graphs clearly depict that the a-b and c-d states are onion-like, while the e-f states have a domain-wall character. For a properly chosen field orientation (Fig. 2b) these states are stabilized, at zero-valued field, in a middle of one sample side. A separate issue is related to the problem of metastability of a domain-wall. However, in a scope of definition of intermediate stable states obtained by a reversible process, we show in

Fig. 4 that the creation of a domain-wall begins not near zero-valued external field, but quite earlier - as it is seen in the figure the e-f domain-wall states represent a global feature of a sample, thus can be understood as the stable ones at remanence.

## IV. CONCLUSION

It was shown that highly symmetric wire systems reveal interesting multilevel state behavior. What is important, postulated shapes and dimensions became accessible by contemporary technological methods, for example nano-imprint lithography.[12] Comparing a previous four-fold system with the actual six-fold one, it is evident that intermediate stable states are much more easily obtainable for a quaternary structure, for wider range of field values and orientations, since this solution was fully based on onion states.[6]

What makes presented wire structures also interesting is that their operational mechanism does not require magnetization fixing. The mechanism is governed by states originating from competing exchange and demagnetizing fields. During simulations we observed two types of possibilities, those based on onion states and those associated with domain walls. Test with different directions of externally applied magnetic field suggests that onion states have higher stability for the wider range of field directions, while domain walls can be obtained only for specific field orientations. The higher remanences of the obtained onion states are compatible with their stability. A stability of domain wall states results from their dynamics - they are based on domain wall propagation along a wire, for a given value and orientation of externally applied magnetic field. The onion states, on the other hand, are fixed at vertexes. The presented phenomena will be intensively studied in future, especially in order to test stability of the remanent states. Additionally, conceptions of *n*-fold symmetrical wire samples, with $n > 6$, require systematic studies.

## ACKNOWLEDGEMENT

The authors acknowledge partial project funding by Niederrhein University of Applied Sciences.

[1] R. Sbiaa, S. Y. H. Lua, R. Law, H. Meng, R. Lye, and H. K. Tan, J. Appl. Phys. **109**, 07C707 (2011).

[2] T. Blachowicz, A. Tillmanns, M. Fraune, R. Ghadimi, B. Beschoten, and G. Güntherodt, Phys. Rev. B **75,** 054425 (2007).

[3] N. Thiyagaraja, K.-I. Lee[2], and S. Bae, J. Appl. Phys. **111**, 07C910 (2012).

[4] W.-Ch. Jeong, B.-I. Lee, and S.-K. Joo, IEEE Trans. Magn. **34**, 1069 (1998).

[5] W.-Ch. Jeong, B.-I. Lee, and S.-K. Joo, J. Appl. Phys. **85**, 4782 (1999).

[6] T. Blachowicz and A. Ehrmann, J. Appl. Phys. **110**, 073911 (2011).

[7] J. C. Slonczewski, J. Mag. Magn. Mat. **247**, 324 (2002).

[8] W. Scholtz, J. Fidler, T. Schrefl, D. Suess, R. Dittrich, H. Forster, and V. Tsiantos, Comp. Mater. Sci. **28**, 366 (2003).

[9] L. Thevenard, H. T. Zeng, D. Petit, and R. P. Cowburn, J. Magn. Magn. Mater. **322**, 2152 (2010).

[10] S. Tehrani, B. Engel, J. M. Slaughter, E. Chen, M. DeHerrera, M. Durlam, P. Naji, R. Whig, J. Janesky, and J. Calder, IEEE Trans. Magn. **36**, 2752 (2000).

[11] K. J. Harte, J. Appl. Phys. J. Appl. Phys. **39**, 1503 (1968).

[12] G. L. W. Cross, J. Phys. D: Appl. Phys. **39**, R363 (2006).

**Figure captions**

Fig. 1. The iron six-fold (hexagonal) sample constructed from wires (half-circle at cross-section) of 70 nm length and 10 nm width, and half-balls of 20 nm base-diameter (a). The $\alpha$ angle defines the external magnetic field vector orientation. At the corner the base-planes of wires are 1 nm up-shifted with respect to the half-ball base-plane, in order to induce additional demagnetizing fields stabilizing magnetic states at remanence (b).

Fig. 2. Externally applied magnetic field sequence (a) and hysteresis curves for three different magnetic field orientations: (b) α=35° giving 3-level, 6-state possibility, and (c) α=46° losing domain-wall states completely. Arrows indicate directions of external field changes equivalent to the sequence given in figure (a).

Fig. 3. (color online) The six stable magnetic states at remanence (comp. Fig. 2b): the onion states (a, b, c, d) and the domain-wall states stabilized at middle positions of wires (e, f). Colors of samples code the $M_x$ component of the magnetization vector: the component parallel to x-axis direction $M_x$=1 (red), the component anti-parallel to x-axis direction $M_x$=-1 (blue), and the component perpendicular to x-axis $M_x$=0 (green). The external field direction $H_{ext}$ is sketched.

Fig. 4. (color online) The evolution of the domain-wall e-state: creation of a domain-wall begin for $H_{ext}$=96 kA/m (1.), leads to the e-state at $H_{ext}$=0 kA/m (5.), and is finished for $H_{ext}$=169 kA/m (7.). The inset shows subsequent states of one sample arm - colors code the $M_x$ component of the magnetization vector: the component parallel to x-axis direction $M_x$=1 (red), the component anti-parallel to x-axis direction $M_x$=-1 (blue), and the component perpendicular to x-axis $M_x$=0 (green).

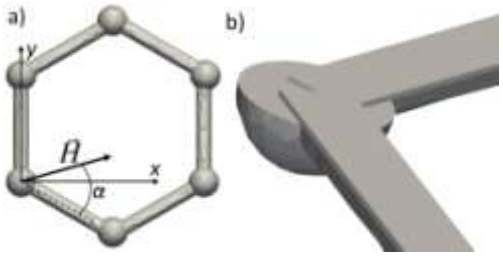


Fig. 1.

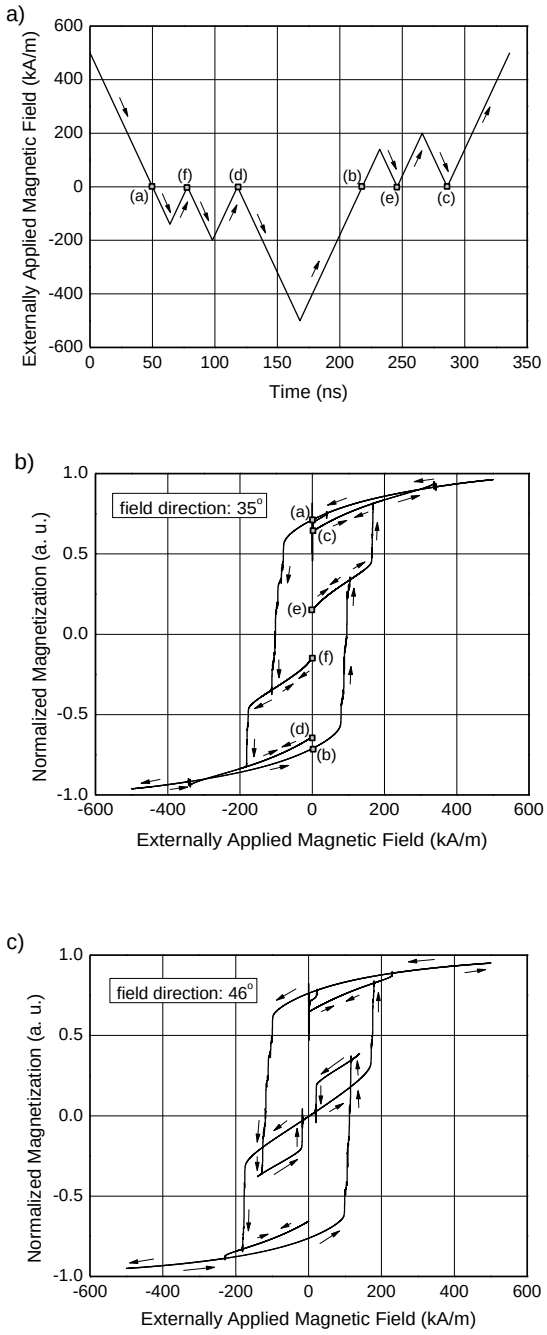
a)
Externally Applied Magnetic Field (kA/m)
Time (ns)
(a)
(f)
(d)
(b)
(e)
(c)
b)
field direction: 35°
Normalized Magnetization (a. u.)
Externally Applied Magnetic Field (kA/m)
c)
field direction: 46°
Normalized Magnetization (a. u.)
Externally Applied Magnetic Field (kA/m)

Fig. 2.

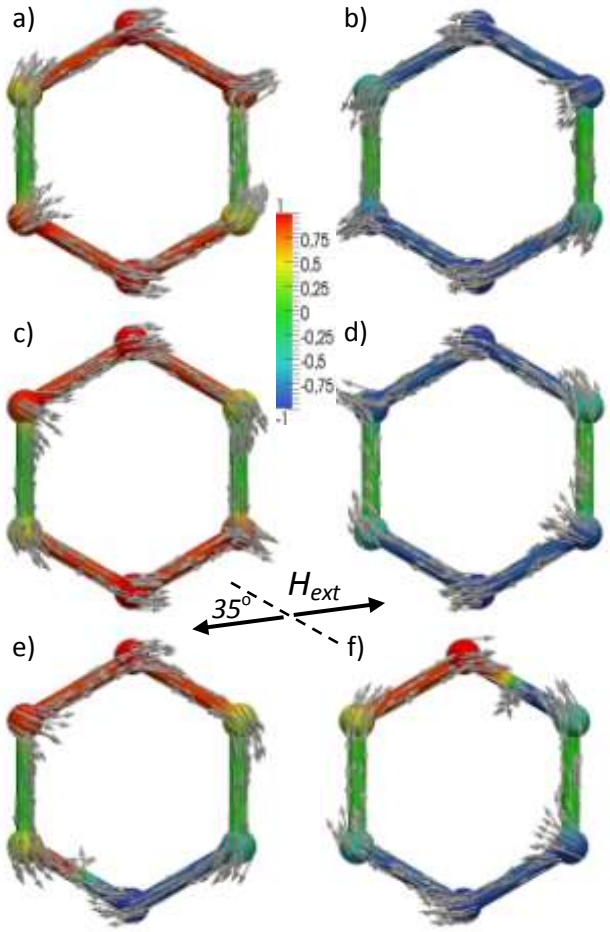


Fig. 3.

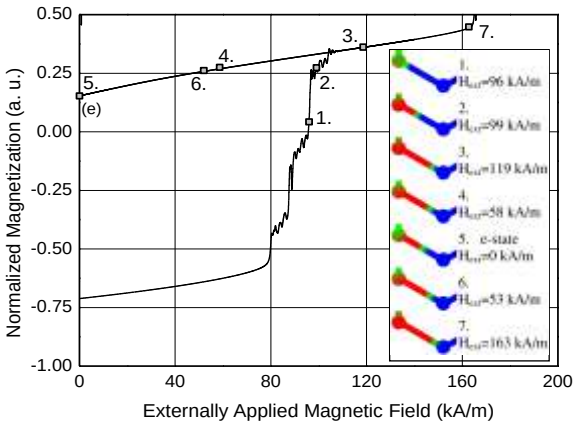
0.50
0.25
0.00
-0.25
-0.50
-0.75
-1.00
Normalized Magnetization (a. u.)
0
40
80
120
160
200
Externally Applied Magnetic Field (kA/m)
1.
2.
3.
4.
5.
6.
7.
(e)
1.
2.
3.
4.
5. e-state
6.
7.

Fig. 4.